Effect of the Addition of Re on the Microstructure and Phase Composition of Haynes 282: Ab Initio Modelling and Experi-Mental Investigation of Additively Manufactured Specimens

Antoni Wadowski , Jan S. Wróbel , Milena Koralnik , Ryszard Sitek *

Posted Date: 6 May 2023

doi: 10.20944/preprints202305.0411.v1

Keywords: ab initio calculation; short-range ordering; rhenium effect; nickel alloys; additive manufacturing

Article

Effect of the Addition of Re on the Microstructure and Phase Composition of Haynes 282: Ab Initio Modelling and Experimental Investigation of Additively Manufactured Specimens

Antoni Wadowski, Jan S. Wróbel, Milena Koralnik and Ryszard Sitek *

Faculty of Materials Science and Engineering, Warsaw University of Technology, Wołoska 141, 02-507 Warsaw, Poland

* Correspondence: ryszard.sitek@pw.edu.pl; Tel.: +48 022 234 81 57; fax: +48 022 234 81 08

Abstract: Interactions in multicomponent Ni-Cr-Mo-Al-Re model alloy were determined by ab initio calculations in order to investigate the Re doping effect on Haynes 282 alloy. Simulation results provided an understanding of short-range interactions in the alloy and successfully predicted the formation of a Cr and Re-rich phase. The Haynes 282 + 3 % wt. Re alloy was manufactured using the additive manufacturing Direct Metal Laser Sintering (DMLS) technique, in which the presence of the $(Cr_{17}Re_6)C_6$ carbide was confirmed by an XRD study. The results obtained provide useful information about the interactions between Ni, Cr, Mo, Al, and Re as a function of temperature. The 5-element model designed can lead to a better understanding of phenomena that occur during the manufacturing or heat treatment of modern, complex, multicomponent Ni-based superalloys.

Keywords: ab initio calculation; short-range ordering; rhenium effect; nickel alloys; additive manufacturing

1. Introduction

Ni-based superalloys are widely used in the aviation and power generation industries because of their excellent mechanical properties, which are maintained even at high temperatures, and because of their good oxidation resistance and manufacturability. In order to further improve the efficiency of turbines, materials are needed that can withstand extreme temperatures during service under severe stresses and corrosive environment. This can be achieved by optimising the chemical composition of the alloy.

One such superalloy is Haynes 282, whose chemical composition was designed to achieve a desirable combination of strength, thermal stability and fabricability [1]. Like other gamma' strengthened Ni-based superalloys, Haynes 282 acquires its mechanical properties by: (i) precipitation of the gamma' phase (addition of Al and Ti), (ii) solid solution strengthening (Cr, Co, Mo), and (iii) the presence of carbides and borides.

By optimising the Al and Ti content of Haynes 282, the volume fraction of the gamma' phase is relatively low (19 % in fully-aged condition); this is in order to prevent the phenomenon of strain-age cracking [1] and to achieve good weldability. The impact of a lower volume fraction of gamma' is offset by the addition of 8.5 wt. % Mo, which plays an important role in maintaining high creep strength through solid solution strengthening, especially near the higher end of the anticipated temperature range [2]. The alloy's good weldability means it lends itself to additive manufacturing (AM) by powder bed fusion, which opens up new possibilities for designing parts and material microstructure.

Rhenium as an alloying element increases the creep properties [3–7], fatigue strength, oxidation and corrosion resistance [4] of Ni-based superalloys. After a debate over the mechanisms underlying the Re effect, it was shown that the improvement in creep strain rate results directly from Re

Preprints (www.preprints.org) | NOT PEER-REVIEWED | Posted: 6 May 2023 doi:10.20944/preprints202305.0411.v1

enrichment to partial dislocations, hindering their movement [8]. Besides its direct interactions with dislocations, Re significantly enhances the stability of gamma' precipitates and suppresses variations in composition within the gamma matrix [9]. Re atoms, which have the lowest diffusion coefficient in Ni-based superalloys, slow down diffusion-controlled processes in the microstructure, therefore increasing its stability during exposure to high temperatures [4,9]. It has been shown that Re atoms enrich gamma dendrites in multicomponent Ni alloys [7,10–14], leading to a nonhomogeneous distribution of elements between the dendritic and interdendritic regions. Moreover, Re leads to the formation of TCP phases, which are harmful to high-temperature properties [4,5,11,15,16]. Although Re's tendency to microsegregation [7,10–14] and crystal lattice occupying sites [17] are well established, a quantitative analysis of Re's interactions in multicomponent Ni-based superalloys requires a more thorough examination. This knowledge is necessary to further enhance the properties of Ni-based superalloys by optimising their chemical composition.

The aim of this study was to improve our knowledge of the interactions between atoms and phase stability in rhenium-doped additively manufactured Haynes 282 alloy, resulting in a modification of its mechanical properties. The Haynes 282 + 3 % wt. Re was manufactured by means of Direct Metal Laser Sintering (DMLS).

2. Materials and Methods

To investigate the effect of adding Re to Haynes 282 alloy, the cluster expansion model for the face-centred cubic (fcc) Ni-Cr-Mo-Al-Re system was developed, in which the effective cluster interactions were determined based on Density Functional Theory (DFT). Simulations for systems with different chemical compositions (Table 1) were carried out. To reflect Haynes 282 properties by fife element cluster expansion model, the most important alloy elements were chosen: Ni, Cr, Mo and Al. Chromium and molybdenum are amongst the most abundant elements in the Haynes 282 and their fraction corresponded to the reference alloy's composition [1]. It is worth noting that there is a higher percentage of Co than Mo in Haynes 282 (10 and 8.5 wt. % respectively). However, molybdenum was chosen to be included in the model. It plays an important role in defining creep properties of Haynes 282 [1], while also having an influence on the phase stability of Ni-based superalloys, i.e., leading to μ phase formation [18]. Because both Al and Ti mainly enrich gamma' $L1_2$-$Ni_3(Al,Ti)$ phase in Ni-based superalloys [19] and occupy similar positions in its crystal structure [17], the concentration of Al was set as a sum of Al and Ti fraction in Haynes 282 alloy. Other elements present in the reference alloy (i.e.,: Co, Fe, Mn) were fully replaced by Ni. In subsequent variations (Table 1), Re was added at the expense of wt. % of Ni, which imitated experimental Re doping of Haynes 282 powder.

Table 1. Chemical compositions of investigated Ni-Cr-Al-Re alloy models.

wt. % of Re	0	3	6	9
Ni [at. %]	65	64	62	61
Cr [at. %]	22	22	23	23
Mo [at. %]	5	5	5	5
Al [at. %]	8	8	8	8
Re [at. %]	0	1	2	3

DFT calculations were performed using Vienna Ab initio Simulation Package (VASP) [20,21] with cutoff energy equal to 400 eV and the Monkhorst-Pack mesh [22] of *k* points in the Brillouin zone, with *k*-mesh spacing of 0.2 °A−1, which corresponds to 12×12×12
k-point meshes for a four-atom fcc cubic cell. The total energies were converged to 10^{-5} eV and the force components in calculations involving full cell relaxation were relaxed to
10^{-3} eV/Å. Alloy Theoretic Automated Toolkit (ATAT) [23] was used to develop the cluster expansion (CE) model for the fcc Ni-Cr-Mo-Al-Re system based on DFT calculations for 403 binary, 771 ternary and 494 quaternary structures. In the CE formalism, the enthalpy of mixing of an alloy described by a vector of the configurational variables, $\vec{\sigma}$, was expressed as [23–25]

Preprints (www.preprints.org) | NOT PEER-REVIEWED | Posted: 6 May 2023 doi:10.20944/preprints202305.0411.v1

$$H_{mix}(\vec{\sigma}) = \sum_{\omega} m_{\omega} J_{\omega} \langle \Gamma_{\omega'}(\vec{\sigma}) \rangle \quad (1)$$

where summation is preformed over all the clusters ω, with multiplicity m_ω. J_ω are concentration independent effective cluster interaction parameters (ECIs) and $\langle \Gamma_{\omega'}(\vec{\sigma}) \rangle$ are cluster functions defined as products of point functions of occupation variables on a specific cluster ω averaged over all the clusters ω' that are equivalent to the cluster ω by symmetry. In the CE model for the fcc Ni-Cr-Mo-Al-Re system, we used 50 two-body, 100 three-body and 35 four-body ECIs. The cross-validation score between the enthalpies of mixing computed using DFT and CE was 22.3 meV. In order to investigate the phase stability of fcc Ni-Cr-Mo-Al-Re alloys, the CE model was next applied in Monte Carlo (MC) simulations, which were conducted using the ATAT code [23] by quenching the system from the temperature 2000 K to 200 K with a temperature step equal to 100. Simulation cells were 20 x 20 x 20 fcc unit cell, containing 8000 atoms. The correlation functions and enthalpies of mixing were calculated by averaging the MC results over 2000 MC steps per atom at each temperature.

The chemical ordering in alloys was investigated by the calculation of the Warren-Cowley short-range order (SRO) parameters, defined as

$$\alpha_n^{ij} = 1 - \frac{y_n^{ij}}{c_i c_j} \quad (2)$$

where i and j are the n-th nearest neighbour atoms, c_i and c_j are the concentrations of atoms i and j, respectively, and y_n^{ij} is the average pair probability, which can be obtained from the average point and pair correlation function as in Refs. [25–27].

Samples of the modified alloy were manufactured using the DMLS technique. To obtain a powder of Haynes 282 + 3% mass Re, an unmodified alloy was mixed with 99,99 % Re powder in a mass proportion of 50/50. The materials were mixed in a planetary grinder and then pure Haynes 282 powder was added to achieve a mixture of Haynes 282 with 3 % mass Re. The 10x20x15 mm samples were manufactured using EOS M100 3D printer. This operation was followed by a standard heat treatment for Haynes 282. Firstly, solution annealing at 1149 °C for 2 h followed by water-quenching was carried out. Then samples were subjected to two-stage age-hardening treatment: 1010 °C for 2 h air cooled and 788 °C for 8 h air cooled.

Phase analysis of the investigated material was performed by means of X-ray diffraction (XRD) at room temperature using a Bruker D8 Advance diffractometer with filtered CuKα radiation (λ = 0.154056 nm). The results were recorded by stepwise scanning in a 2Θ range of 20°÷120°, with a step size of 0.05°, a count time of 3 s per step, and a voltage of 40 kV. The XRD patterns were analyzed using Bruker EVA software and a PDF-2 database.

3. Results and Discussion

3.1. Ab-initio Modelling

As shown in Figure 1a, the addition of Re to Haynes 282 practically did not change the alloy's enthalpy of mixing for temperatures below 1200 K. In higher temperatures enthalpy of mixing increases with the Re concentration in the alloy. An order-disorder transformation also occurred at the same temperature (approximately 1450 K).

Preprints (www.preprints.org) | NOT PEER-REVIEWED | Posted: 6 May 2023 doi:10.20944/preprints202305.0411.v1

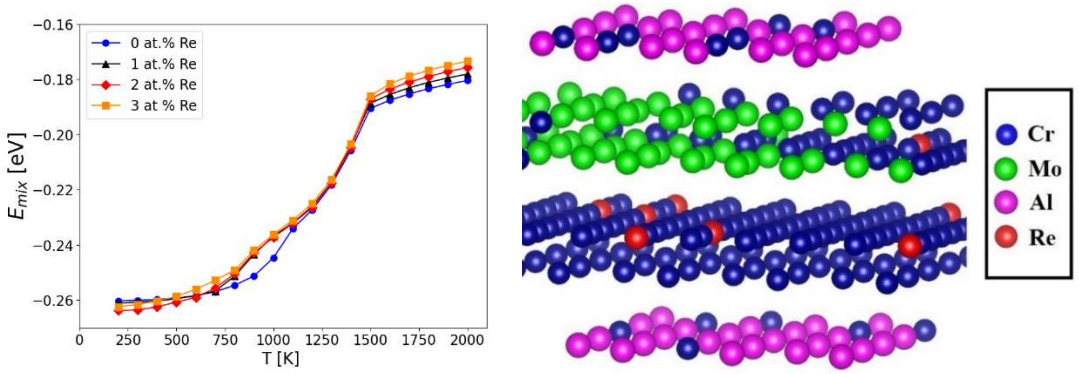

(**a**) (**b**)

Figure 1. (a) Enthalpies of mixing (Emix) for alloys with the chemical compositions listed in Table 1 and (b) Ni64Cr22Mo5Al8Re1 structure visualisation (which correspond to Haynes 282 + 3 % mas. Re, listed in Table 1), at a temperature of 300 K. Ni atoms were excluded from a visualisation for clarity.

In Figure 1b, there is shown a representative structure of the alloy containing 1 at. % Re generated using MC simulations at 300 K. There are visible regions with the coexistence of Cr and Re atoms as well as the coexistence of Al and Cr atoms.

In order to study the atomic ordering in Ni-Cr-Mo-Al-Re alloys as a function of Re concentration and temperature, the SRO parameters were calculated using Equation (2) based on average correlation functions from MC simulations. The values of SRO for the pairs of atoms in the 1st and 2nd nearest neighbour coordination shell are shown in Figures 2 and 3, respectively.

The lower and more negative the SRO value, the stronger the attractive forces between pairs of atoms, and vice versa. Therefore, systems with a lower SRO interactions value are more likely to create disordered - or when the SRO is significantly low - even ordered solid solutions. Increasing and positive the SRO value means stronger repulsive forces between pairs of atoms, leading to the segregation of the mixture.

As presented in Figure 2a, the values of SRO parameters for the 1st nearest neighbour coordination shell ($\alpha 1$) are strongly negative for the Cr-Re system throughout the investigated temperature range. The forces between the Cr and Re atoms can cause the formation of stable ordered structures, such as intermetallic phases. Effect of attractive forces between Cr and Re atoms can be seen in Figure 1b, in which Re is distributed in the direct neighbourhood of the Cr atoms.

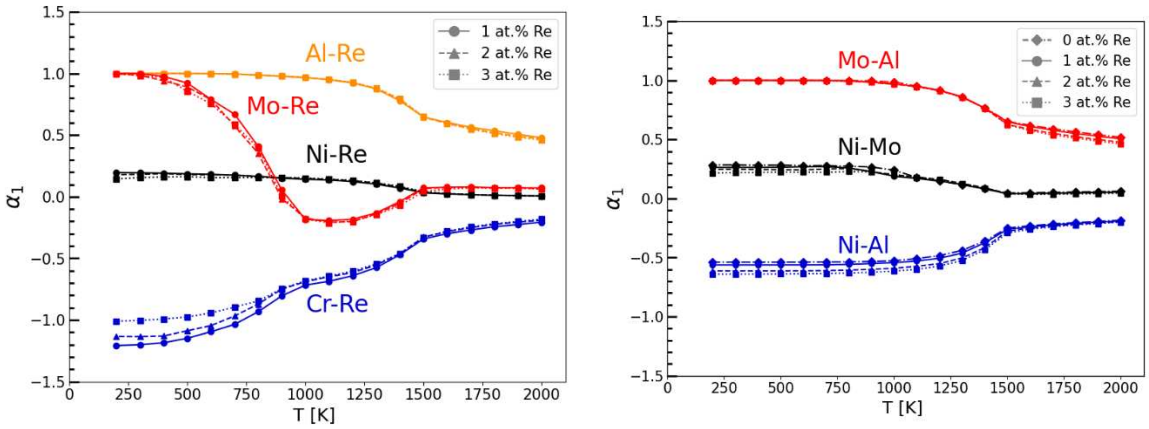

(**a**) (**b**)

Preprints (www.preprints.org) | NOT PEER-REVIEWED | Posted: 6 May 2023 doi:10.20944/preprints202305.0411.v1

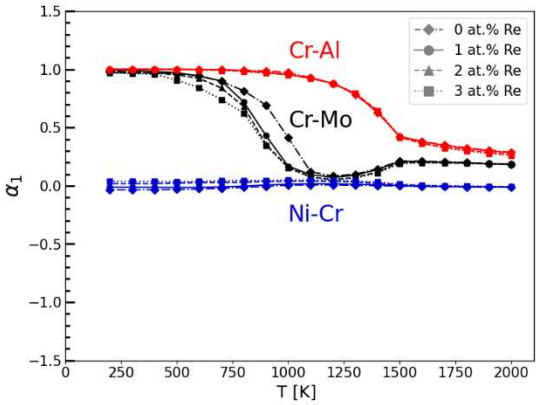

(c)

Figure 2. Calculated short-range order (SRO) parameters for pairs of atoms in the 1st nearest neighbour coordination shell (α_1): a) Re and X atoms, where X = {Ni, Cr, Mo, Al}, b) Ni-Mo, Ni-Al, Mo-Al and c) Cr-Al, Cr-Mo, Ni-Cr pairs.

Interactions of other pairs of atoms (Al-Re, Mo-Re, Ni-Re) have positive values of $\alpha 1$ throughout the temperature range, except for the Mo-Re pair. At temperatures near 1100 K, the $\alpha 1$ values for the Mo and Re atoms have slightly negative values. This suggests that during alloy exposure at that temperature (i.e., during casting or heat treatment), it is possible for phases rich in Mo and Re to precipitate. The $\alpha 1$ characteristic of the Ni-Re pair indicates that, because of slightly positive values, lower than 0.25, Ni and Re create a disordered solid solution, whose elements show little tendency to segregate.

Based on the modelling results, it is suspected that Al and Re would strongly segregate form one another. Therefore Re is not supposed to be present within an ordered gamma' $L1_2$ Ni_3Al structure (see Figure 1b). As shown in Figure 2b, the α_1 values for the Ni-Al system were the lowest of the atomic Al pairs investigated, making this element the one most likely to exist in phases with Ni. This is a common observation and remains the basic principle behind nickel superalloys' precipitation strengthening.

Furthermore, because of high values of α_1 in systems Mo-Al (Figure 2b) and Cr-Al (Figure 2c) it can be concluded that Mo and Cr would not occur in 1st nearest neighbour positions of Al.

As presented in Figure 3a, the values of SRO parameters for the 2nd nearest neighbour coordination shell (α_2) for Re and other elements present in the model (Ni, Cr, Mo and Al) show a similar tendency to the results for 1st shell (Figure 2a). However, for 2nd shell SRO parameter for Mo-Re have more negative values in a broader temperature range. The α_2 for Ni-Al presented in the Figure 3b have positive values. This suggests that Ni and Al atoms will not be likely to present in their 2nd neighbourhood positions. This observation is in good agreement with the structure of the ordered gamma' $L1_2$ Ni_3Al phase present in Haynes 282. It can be seen that in the case of the Cr-Al pair SRO parameter for the 2nd nearest neighbour coordination shell (see Figure 3c) have negative values, contrary to the results for 1st shell (Figure 2c). In effect, some Cr can be present near Al atoms (see Figure 1b), preferably in their 2nd nearest neighbour position. The addition of Re significantly reduces this tendency, leading to less negative α_2 for Cr-Al system.

Preprints (www.preprints.org) | NOT PEER-REVIEWED | Posted: 6 May 2023 doi:10.20944/preprints202305.0411.v1

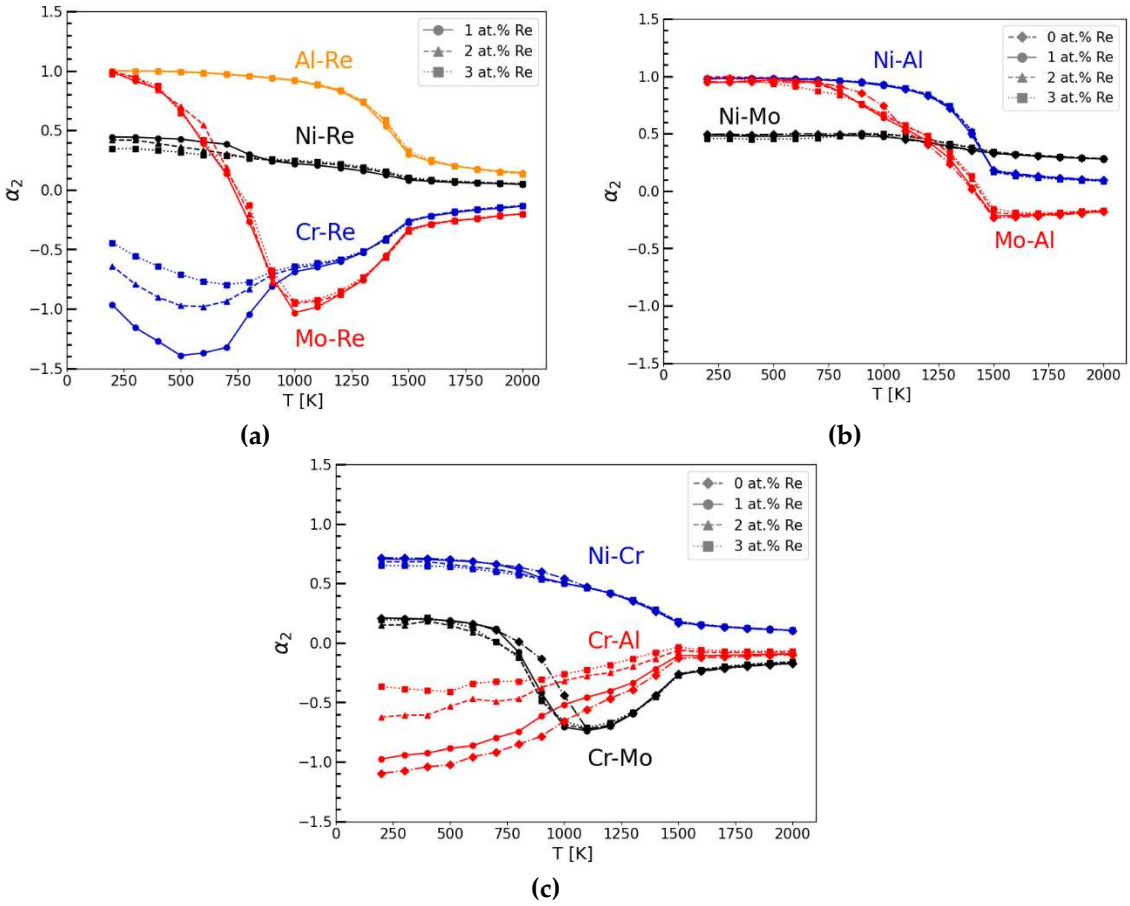

Figure 3. Calculated SRO parameters for pairs of atoms in 2nd nearest neighbour coordination shell (α_2) : a) Re and X atoms, where X = {Ni, Cr, Mo, Al}, b) Ni-Mo, Ni-Al, Mo-Al and c) Cr-Al, Cr-Mo, Ni-Cr pairs.

3.2. XRD Results and Comparison with MC Simulations

Figure 4 shows a diffraction pattern of the material examined along the Z-axis of a printed sample with the pattern of the $Ni_3(Al_{0.5}Ti_{0.5})$ phase in the matrix solution of Ni and Cr. A broadening of the major diffraction peaks was observed, probably due to the presence of additional phases. Based on the positions of the diffraction peaks and the known chemical composition of the tested material, and using the PDF-2 database, the $Al_{0.05}Cr_{0.3}Ni_{0.65}$ and $C_6(Cr_{17}Re_6)$ phases were characterized by the highest degree of adjustment. The identified phases show a cubic crystal system with lattice parameters of 3.566 Å and 10.890 Å, respectively. The tests performed did not reveal the presence of Mo-containing phases.

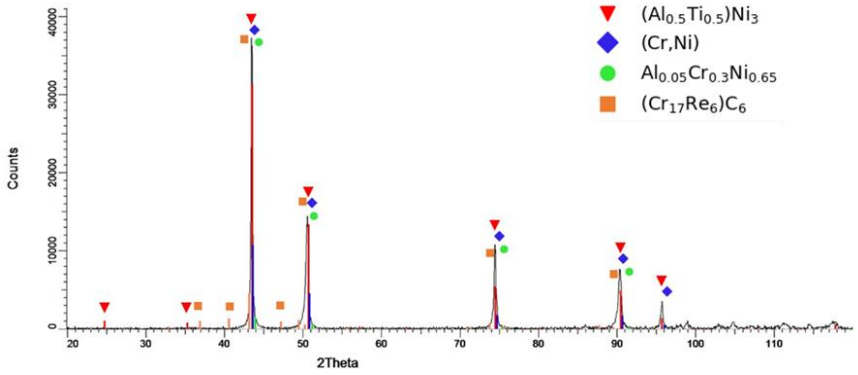

Figure 4. X-ray diffractogram pattern of Haynes 282 + 3 wt. % Re.

The existence of the Cr- and Re-rich $C_6(Cr_{17}Re_6)$ phases in the considered Ni-based alloy agrees with the Monte Carlo results showing a strong attraction of Cr and Re atoms. It should be noted the theoretical investigation of the alloy stability in the presence of carbon was out of the scope of this work. However, the Monte Carlo simulations show that the Cr- and Re-rich phases should be formed even without C.

Moreover, the presence of $Al_{0.05}Cr_{0.3}Ni_{0.65}$ phase confirms further the Monte Carlo results obtained for the investigated alloy. Unveiled significant attractive forces between Cr and Al atoms in the 2nd nearest neighbour coordination shell can explain formation of stable phase rich in those elements.

4. Conclusions

To conclude, the addition of Re as an alloying element to Haynes 282 preserves the character of the atomic interactions between the most important elements in the alloy, such as Ni, Cr, Mo and Al. Therefore, Haynes 282 can be modified with Re to achieve desirable properties that are maintained during heat treatment procedures, similar to those of an unmodified alloy. Additionally, the interactions between elements in the Ni-Cr-Mo-Al-Re system investigated by the MC simulations can help to extend our knowledge about the nature of the interactions between atoms in solution strengthened Ni-based alloys, such as Haynes 282. To the authors' knowledge, the Ni-Cr-Mo-Al-Re alloys have never been investigated using a combination of density functional theory, cluster expansion method and Monte Carlo simulations. The theoretical multicomponent model of the alloy successfully predicted the formation of the phases rich in Re and Cr. $(Cr_{17}Re_6)C_6$ carbide, which was detected later in the XRD study. Moreover, the negative values of SRO parameters for Al-Cr pair in the 2nd nearest neighbour coordination shell explained the presence of $Al_{0.05}Cr_{0.3}Ni_{0.65}$ phase in the X-ray diffractogram pattern of Haynes 282 + 3 wt. %Re.

Author Contributions: Conceptualization, R.S., A.W. and J.W.; ab-initio modelling and comparison of XRD results with MC simulations, A.W. and J.W.; XRD (methodology and interpretation of diffractogram), M.K.; validation and formal analysis, J.W. and R.S.; investigation, A.W., J.W., M.K. and R.S.; data curation, A.W. and J.W; writing—original draft preparation, A.W.; writing—review and editing, J.W., R.S.; visualization, A.W.; resources, supervision, project administration, funding acquisition, R.S., J.W. All authors have read and agreed to the published version of the manuscript.

Funding: Research was funded by POB Technologie Materiałowe of Warsaw University of Technology within the Excellence Initiative: Research University (IDUB) programme.

Data Availability Statement: Data are contained within this article.

Acknowledgments: The simulations were carried out with the support of the Interdisciplinary Centre for Mathematical and Computational Modelling (ICM), University of Warsaw, under grant No. GB79-6.

Conflicts of Interest: The authors declare no conflict of interest.

References

1. Pike, L.M. Development of a Fabricable Gamma-Prime (γ′) Strengthened Superalloy. *Proceedings of the International Symposium on Superalloys* **2008**, 191–200, doi:10.7449/2008/SUPERALLOYS_2008_191_200.
2. Kruger, K.L. HAYNES 282 Alloy. In *Materials for Ultra-Supercritical and Advanced Ultra-Supercritical Power Plants*; Woodhead Publishing, 2017; pp. 511–545 ISBN 9780081005583.
3. Liu, C.P.; Zhang, X.N.; Ge, L.; Liu, S.H.; Wang, C.Y.; Yu, T.; Zhang, Y.F.; Zhang, Z. Effect of Rhenium and Ruthenium on the Deformation and Fracture Mechanism in Nickel-Based Model Single Crystal Superalloys during the in-Situ Tensile at Room Temperature. *Materials Science and Engineering: A* **2017**, *682*, 90–97, doi:10.1016/J.MSEA.2016.10.107.
4. Huang, M.; Zhu, J. An Overview of Rhenium Effect in Single-Crystal Superalloys. *Rare Metals* **2016**, *35*, 127–139, doi:https://doi.org/10.1007/s12598-015-0597-z.
5. Yu, X.X.; Wang, C.Y.; Zhang, X.N.; Yan, P.; Zhang, Z. Synergistic Effect of Rhenium and Ruthenium in Nickel-Based Single-Crystal Superalloys. *J Alloys Compd* **2014**, *582*, 299–304, doi:10.1016/J.JALLCOM.2013.07.201.

6. Neumeier, S.; Pyczaky, F.; Göken, M. Influence of Rhenium and Ruthenium on the Local Mechanical Properties of the γ and γ′ Phases in Nickel-Base Superalloys. *Philosophical Magazine* **2011**, *91*, 4187–4199, doi:10.1080/14786435.2011.607139.
7. Heckl, A.; Rettig, R.; Singer, R.F. Solidification Characteristics and Segregation Behavior of Nickel-Base Superalloys in Dependence on Different Rhenium and Ruthenium Contents. *Metall Mater Trans A Phys Metall Mater Sci* **2010**, *41*, 202–211, doi:https://doi.org/10.1007/s11661-009-0076-y.
8. Wu, X.; Makineni, S.K.; Liebscher, C.H.; Dehm, G.; Rezaei Mianroodi, J.; Shanthraj, P.; Svendsen, B.; Bürger, D.; Eggeler, G.; Raabe, D.; Gault B. Unveiling the Re Effect in Ni-Based Single Crystal Superalloys. *Nature Communications 2020 11:1* **2020**, *11*, 1–13, doi:10.1038/S41467-019-14062-9.
9. Zhang, J.; Huang, T.; Lu, F.; Cao, K.; Wang, D.; Zhang, J.; Zhang, J.; Su, H.; Liu, L. The Effect of Rhenium on the Microstructure Stability and γ/Γ′ Interfacial Characteristics of Ni-Based Single Crystal Superalloys during Long-Term Aging. *J Alloys Compd* **2021**, *876*, 160114, doi:10.1016/J.JALLCOM.2021.160114.
10. Zhang, Z.; Wen, Z.; Yue, Z. Effects of Re on Microstructure Evolution of Nickel-Based Single Crystal Superalloys. *Appl Phys A Mater Sci Process* **2020**, *126*, 1–12, doi:10.1007/S00339-020-03864-0.
11. Xia, W.; Zhao, X.; Yue, Q.; Xuan, W.; Pan, Q.; Wang, J.; Ding, Q.; Bei, H.; Zhang, Z. Competitive Deformation Induced by TCP Precipitation and Creep Inconsistency on Dendritic Structures in a Nickel-Based Single Crystal Superalloy Crept at High Temperatures. *Mater Charact* **2022**, *187*, 111855, doi:10.1016/J.MATCHAR.2022.111855.
12. Petrushin, N. v.; Elyutin, E.S.; Nazarkin, R.M.; Pakhomkin, S.I.; Kolodochkina, V.G.; Fesenko, T. v.; Dzhioeva, E.S. Segregation of Alloying Elements in Directionally Solidified Re–Ru-Containing Ni-Based Superalloys. *Inorganic Materials: Applied Research 2016 7:6* **2016**, *7*, 824–831, doi:10.1134/S2075113316060149.
13. Liu, E.; Guan, X.; Zheng, Z. Effect of Rhenium on Solidification and Segregation of Nickel-Based Superalloy. *Rare Metals 2011 30:1* **2011**, *30*, 320–322, doi:10.1007/S12598-011-0294-5.
14. Lopez-Galilea, I.; Koßmann, J.; Kostka, A.; Drautz, R.; Mujica Roncery, L.; Hammerschmidt, T.; Huth, S.; Theisen, W. The Thermal Stability of Topologically Close-Packed Phases in the Single-Crystal Ni-Base Superalloy ERBO/1. *J Mater Sci* **2016**, *51*, 2653–2664, doi:10.1007/S10853-015-9579-7.
15. Sun, N.; Zhang, L.; Li, Z.; Shan, A. The Effect of Microstructure on the Creep Behavior of a Low Rhenium-Containing Single Crystal Nickel-Based Superalloy. *Materials Science and Engineering: A* **2014**, *606*, 175–186, doi:10.1016/J.MSEA.2014.03.074.
16. Sun, N.; Zhang, L.; Li, Z.; Shan, A. Effect of Heat-Treatment on Microstructure and High-Temperature Deformation Behavior of a Low Rhenium-Containing Single Crystal Nickel-Based Superalloy. *Materials Science and Engineering: A* **2014**, *606*, 417–425, doi:10.1016/J.MSEA.2014.03.093.
17. Eriş, R.; Akdeniz, M.V.; Mekhrabov, A.O. The Site Preferences of Transition Elements and Their Synergistic Effects on the Bonding Strengthening and Structural Stability of γ′-Ni3Al Precipitates in Ni-Based Superalloys: A First-Principles Investigation. *Metall Mater Trans A Phys Metall Mater Sci* **2021**, *52*, 2298–2313, doi:10.1007/S11661-021-06222-8.
18. Yang, Y.; Brutti, S.; Xu, X. Microstructural Evolution of Large Cast Haynes 282 at Elevated Temperature. *Crystals 2021, Vol. 11, Page 867* **2021**, *11*, 867, doi:10.3390/CRYST11080867.
19. Shao, Y. long; Xu, J.; Wang, H.; Zhang, Y. wen; Jia, J.; Liu, J. tao; Huang, H. liang; Zhang, M.; Wang, Z. cheng; Zhang, H. fei; Hu B. fu. Effect of Ti and Al on Microstructure and Partitioning Behavior of Alloying Elements in Ni-Based Powder Metallurgy Superalloys. *International Journal of Minerals, Metallurgy, and Materials 2019 26:4* **2019**, *26*, 500–506, doi:10.1007/S12613-019-1757-1.
20. Kresse, G.; Furthmüller, J. Efficiency of Ab-Initio Total Energy Calculations for Metals and Semiconductors Using a Plane-Wave Basis Set. *Comput Mater Sci* **1996**, *6*, 15–50, doi:10.1016/0927-0256(96)00008-0.
21. Kresse, G.; Furthmüller, J. Efficient Iterative Schemes for Ab Initio Total-Energy Calculations Using a Plane-Wave Basis Set. *Phys Rev B* **1996**, *54*, 11169, doi:10.1103/PhysRevB.54.11169.
22. Monkhorst, H.J.; Pack, J.D. Special Points for Brillouin-Zone Integrations. *Phys Rev B* **1976**, *13*, 5188, doi:10.1103/PhysRevB.13.5188.
23. van de Walle, A.; Asta, M.; Ceder, G. The Alloy Theoretic Automated Toolkit: A User Guide. *Calphad* **2002**, *26*, 539–553, doi:10.1016/S0364-5916(02)80006-2.
24. Sanchez, J.M.; Ducastelle, F.; Gratias, D. Generalized Cluster Description of Multicomponent Systems. *Physica A: Statistical Mechanics and its Applications* **1984**, *128*, 334–350, doi:10.1016/0378-4371(84)90096-7.
25. Wróbel, J.S.; Nguyen-Manh, D.; Lavrentiev, M.Y.; Muzyk, M.; Dudarev, S.L. Phase Stability of Ternary Fcc and Bcc Fe-Cr-Ni Alloys. *Phys Rev B Condens Matter Mater Phys* **2015**, *91*, 024108, doi:10.1103/PHYSREVB.91.024108.
26. Fedorov, M.; Wróbel, J.S.; Fernández-Caballero, A.; Kurzydłowski, K.J.; Nguyen-Manh, D. Phase Stability and Magnetic Properties in Fcc Fe-Cr-Mn-Ni Alloys from First-Principles Modeling. *Phys Rev B* **2020**, *101*, 174416, doi:10.1103/PHYSREVB.101.174416.
27. Fernández-Caballero, A.; Wróbel, J.S.; Mummery, P.M.; Nguyen-Manh, D. Short-Range Order in High Entropy Alloys: Theoretical Formulation and Application to Mo-Nb-Ta-V-W System. *J Phase Equilibria Diffus* **2017**, *38*, 391–403, doi:10.1007/S11669-017-0582-3.

 doi:10.20944/preprints202305.0411.v1